

Turbo Coded Single User Massive MIMO with Precoding

K. Vasudevan, Gyanesh Kumar Pathak, A. Phani Kumar Reddy

Department of Electrical Engineering, Indian Institute of Technology Kanpur-208016, India.

{vasu, pathak, phani}@iitk.ac.in

Summary: Precoding is a method of compensating the channel at the transmitter. This work presents a novel method of data detection in turbo coded single user massive multiple input multiple output (MIMO) systems using precoding. We show via computer simulations that, when precoding is used, re-transmitting the data does not result in significant reduction in bit-error-rate (BER), thus increasing the spectral efficiency, compared to the case without precoding. Moreover, increasing the number of transmit and receive antennas results in improved BER.

Keywords: Precoding, massive MIMO, turbo codes, flat fading, spectral efficiency.

1. Introduction

Precoding at the transmitter is a technique that dates back to the era of voiceband modems or wired communications [1–7]. The term “precoding” is quite generic and refers to one or more of the many different functionalities, as given below:

1. It compensates for the distortion introduced by the channel. Note that channel compensation at the receiver is referred to as equalization [8–14]. Here, channel compensation implies removal or minimization of intersymbol interference (ISI).
2. It performs error control coding, besides channel compensation.
3. It shapes the spectrum of the transmitted signal, and renders it suitable for propagation over the physical channel. Note that most channels do not propagate a dc signal and precoding is used to remove the dc component in the message signal. At this point, it is important to distinguish between a message signal and the transmitted signal.

In the context of wireless multiple input, multiple output (MIMO) systems, the main task of the precoder is to remove interchannel interference (ICI), either for single-user or multi-user case [15–21]. It should be observed that precoding requires knowledge of the channel state information (CSI) at the transmitter, which is usually fed back by the receiver to the transmitter. The receiver estimates CSI from a known training signal that is sent by the transmitter. CSI usually refers to the channel impulse response (CIR) or its statistics (mean and covariance), depending on the type of precoder used. Thus, precoding requires the channel to be time invariant or wide sense stationary (WSS) over at least one transmit and receive duration. Moreover, precoding can only be performed on systems employing time division duplex (TDD), which is a method of half duplex telecommunication. In other words, the channel needs to be reciprocal, that is, the CIR from the

transmitter to receiver must be identical to that from receiver to transmitter.

In this work, we describe an elegant precoding method which reduces ICI in single user massive MIMO systems and compare it with the case without precoding [22, 23]. Rayleigh flat fading channel is assumed. If the channel is frequency selective, orthogonal frequency division multiplexing (OFDM) can be used [14, 23–35].

This work is organized as follows. Section 2 describes the signal model. In Section 3 precoding for single user massive MIMO is discussed. Section 4 presents the simulation results and conclude the work in Section 5.

2. Signal Model

Consider a precoded MIMO system with N_t transmit and N_r receive antennas, as shown in **Fig. 1** [22]. The precoded received signal in the k^{th} ($0 \leq k \leq N_{rt} - 1$, k is an integer), re-transmission is given by

$$\tilde{\mathbf{R}}_k = \tilde{\mathbf{H}}_k \tilde{\mathbf{H}}_k^H \mathbf{S}^p + \tilde{\mathbf{W}}_k \quad (1)$$

where $\tilde{\mathbf{R}}_k \in \mathbb{C}^{N_r \times 1}$ is the received vector, $\tilde{\mathbf{H}}_k \in \mathbb{C}^{N_r \times N_t}$ is the channel matrix and $\tilde{\mathbf{W}}_k \in \mathbb{C}^{N_r \times 1}$ is the additive white Gaussian noise (AWGN) vector. The transmitted symbol vector is $\mathbf{S}^p \in \mathbb{C}^{N_r \times 1}$, whose elements are drawn from an M -ary constellation. Boldface letters denote vectors or matrices. Complex quantities are denoted by a tilde. However tilde is not used for complex symbols \mathbf{S}^p . The elements of $\tilde{\mathbf{H}}_k$ are statistically independent, zero mean, circularly symmetric complex Gaussian with variance per dimension equal to σ_H^2 , as given by (2) of [22]. Similarly, the elements of $\tilde{\mathbf{W}}_k$ are statistically independent, zero mean, circularly symmetric complex Gaussian with variance per dimension equal to σ_W^2 , as given by (3) of [22].

In this work, the elements of \mathbf{S}^p are turbo coded and mapped to a QPSK constellation with coordinates $\pm 1 \pm j$, as depicted in **Fig. 1**. Moreover, here $\tilde{\mathbf{H}}_k$ is an $N_r \times N_t$ matrix, whereas in [22] $\tilde{\mathbf{H}}_k$ is an $N \times N$ matrix. We assume that $\tilde{\mathbf{H}}_k$ and $\tilde{\mathbf{W}}_k$ are independent across re-transmissions, hence (4) in [22]

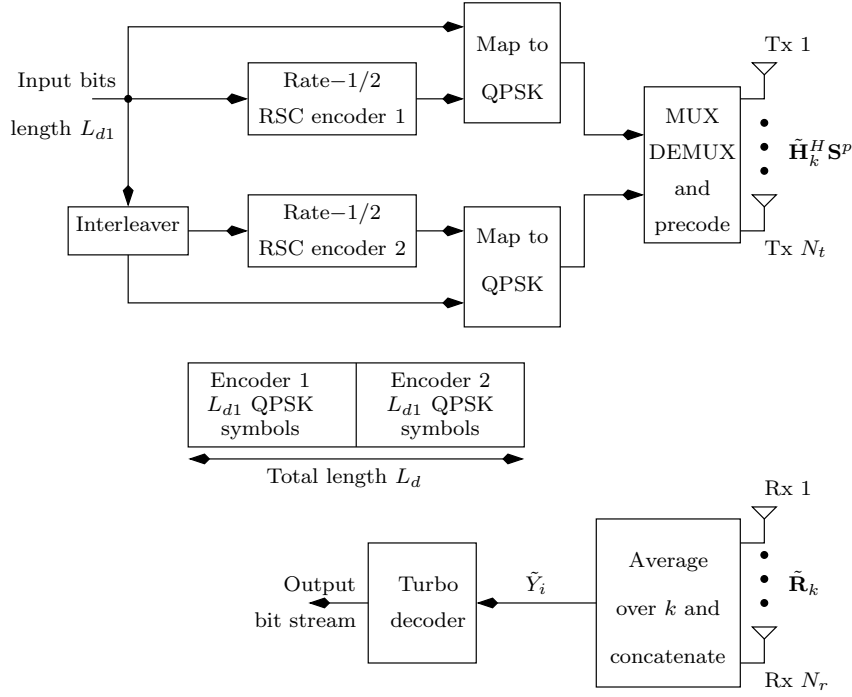


Fig. 1. System model.

is valid with N replaced by N_r . We now proceed to analyze the signal model in (1).

3. Precoding

The i^{th} element of $\tilde{\mathbf{R}}_k$ in (1) is

$$\tilde{R}_{k,i} = \tilde{F}_{k,i} S_i + \tilde{I}_{k,i} + \tilde{W}_{k,i} \quad \text{for } 1 \leq i \leq N_r \quad (2)$$

where

$$\begin{aligned} \tilde{F}_{k,i,i} &= \sum_{j=1}^{N_t} |\tilde{H}_{k,i,j}|^2 \\ \tilde{I}_{k,i} &= \sum_{\substack{j=1 \\ j \neq i}}^{N_r} \tilde{F}_{k,i,j} S_j \\ \tilde{F}_{k,i,j} &= \sum_{l=1}^{N_t} \tilde{H}_{k,i,l} \tilde{H}_{k,j,l}^* \quad \text{for } i \neq j. \end{aligned} \quad (3)$$

The desired signal in (2) is $F_{k,i} S_i$, the interference term is $\tilde{I}_{k,i}$ and the noise term is $\tilde{W}_{k,i}$. Now

$$\begin{aligned} E[\tilde{F}_{k,i,i}^2] &= E\left[\sum_{j=1}^{N_t} |\tilde{H}_{k,i,j}|^2 \sum_{l=1}^{N_t} |\tilde{H}_{k,i,l}|^2\right] \\ &= E\left[\sum_{j=1}^{N_t} \tilde{H}_{k,i,j,I}^2 + \tilde{H}_{k,i,j,Q}^2\right. \\ &\quad \left. \times \sum_{l=1}^{N_t} \tilde{H}_{k,i,l,I}^2 + \tilde{H}_{k,i,l,Q}^2\right] \\ &= 4\sigma_H^4 N_t(N_t + 1) \end{aligned} \quad (4)$$

where the subscript “ I ” denotes the in-phase part and the subscript “ Q ” denotes the quadrature part of a complex quantity and the following relation has been used [36, 37]

$$E[X^4] = 3\sigma_X^4 \quad (5)$$

where X is a zero-mean, real-valued Gaussian random variable with variance σ_X^2 . Moreover from (3) and (2) in [22]

$$E[\tilde{F}_{k,i,i}] = 2\sigma_H^2 N_t. \quad (6)$$

We also have

$$\begin{aligned} E\left[|\tilde{I}_{k,i}|^2\right] &= E\left[\sum_{\substack{j=1 \\ j \neq i}}^{N_r} \tilde{F}_{k,i,j} S_j\right. \\ &\quad \left. \times \sum_{\substack{l=1 \\ l \neq i}}^{N_r} \tilde{F}_{k,i,l}^* S_l^*\right] \\ &= \sum_{\substack{j=1 \\ j \neq i}}^{N_r} \sum_{\substack{l=1 \\ l \neq i}}^{N_r} P_{av} E\left[\tilde{F}_{k,i,j} \tilde{F}_{k,i,l}^*\right] \delta_K(j-l) \\ &= P_{av} \sum_{\substack{j=1 \\ j \neq i}}^{N_r} E\left[|\tilde{F}_{k,i,j}|^2\right] \end{aligned} \quad (7)$$

where $\delta_K(\cdot)$ is the Kronecker delta function [14, 22], we have assumed independence between $\tilde{F}_{k,i,j}$ and S_j and [22]

$$E[S_j S_l^*] = P_{av} \delta_K(j-l)$$

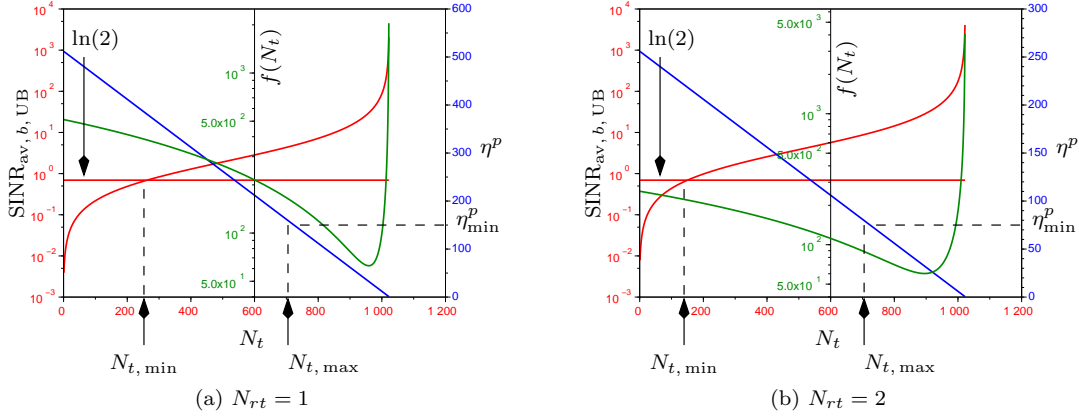


Fig. 2. $\text{SINR}_{\text{av}, b, \text{UB}}$ and η^p as a function of N_t for $N_{\text{tot}} = 1024$.

$$= 2\delta_K(j-l). \quad (8)$$

Now

$$\begin{aligned} E \left[\left| \tilde{F}_{k,i,j} \right|^2 \right] &= E \left[\sum_{l=1}^{N_t} \tilde{H}_{k,i,l} \tilde{H}_{k,j,l}^* \right. \\ &\quad \left. \times \sum_{m=1}^{N_t} \tilde{H}_{k,i,m}^* \tilde{H}_{k,j,m} \right] \\ &= \sum_{l=1}^{N_t} \sum_{m=1}^{N_t} E \left[\tilde{H}_{k,i,l} \tilde{H}_{k,i,m}^* \right] \\ &\quad \times E \left[\tilde{H}_{k,j,m} \tilde{H}_{k,j,l}^* \right] \\ &= \sum_{l=1}^{N_t} \sum_{m=1}^{N_t} 4\sigma_H^4 \delta_K(l-m) \\ &= 4\sigma_H^4 N_t. \end{aligned} \quad (9)$$

Substituting (9) in (7) and using (8) we get

$$E \left[\left| \tilde{I}_{k,i} \right|^2 \right] = 8\sigma_H^4 N_t (N_r - 1). \quad (10)$$

Due to independence between $\tilde{I}_{k,i}$ and $\tilde{W}_{k,i}$ in (2) we have from (10) and (3) of [22]

$$\begin{aligned} E \left[\left| \tilde{I}_{k,i} + \tilde{W}_{k,i} \right|^2 \right] &= E \left[\left| \tilde{I}_{k,i} \right|^2 \right] + E \left[\left| \tilde{W}_{k,i} \right|^2 \right] \\ &= 8\sigma_H^4 N_t (N_r - 1) + 2\sigma_W^2 \\ &= \sigma_U^2, \quad (\text{say}). \end{aligned} \quad (11)$$

Now, each element of \mathbf{S}^p in (1) carries $1/(2N_{rt})$ bits of information [22]. Therefore, each element of $\tilde{\mathbf{R}}_k$ also carries $1/(2N_{rt})$ bits of information. Hence, the average signal to interference plus noise ratio per bit of $\tilde{R}_{k,i}$ in (2) is defined as, using (4), (8) and (11)

$$\text{SINR}_{\text{av}, b} = \frac{E \left[\left| \tilde{F}_{k,i,i} S_i \right|^2 \right] \times 2N_{rt}}{E \left[\left| \tilde{I}_{k,i} + \tilde{W}_{k,i} \right|^2 \right]}$$

$$= \frac{8\sigma_H^4 N_t (N_t + 1) \times 2N_{rt}}{8\sigma_H^4 N_t (N_r - 1) + 2\sigma_W^2}. \quad (12)$$

When $\sigma_W^2 = 0$ in (12), we get the upper bound on $\text{SINR}_{\text{av}, b}$ as given below

$$\begin{aligned} \text{SINR}_{\text{av}, b, \text{UB}} &= \frac{8\sigma_H^4 N_t (N_t + 1) \times 2N_{rt}}{8\sigma_H^4 N_t (N_r - 1)} \\ &= \frac{2N_{rt} (N_t + 1)}{N_r - 1}. \end{aligned} \quad (13)$$

The information contained in \mathbf{S}^p in (1) is $N_r/(2N_{rt})$ bits. Hence the spectral efficiency of the precoded system is

$$\eta^p = \frac{N_r}{2N_{rt}} \quad \text{bits per transmission.} \quad (14)$$

Note that both (13) and (14) need to be as large as possible to minimize the BER and maximize the spectral efficiency. Let

$$N_{\text{tot}} = N_t + N_r. \quad (15)$$

Define

$$\begin{aligned} f(N_t) &= \text{SINR}_{\text{av}, b, \text{UB}} + \eta^p \\ &= \frac{2N_{rt}(N_t + 1)}{N_r - 1} + \frac{N_r}{2N_{rt}} \\ &= \frac{2N_{rt}(N_t + 1)}{N_{\text{tot}} - N_t - 1} + \frac{N_{\text{tot}} - N_t}{2N_{rt}} \end{aligned} \quad (16)$$

where we have used (15). We need to find N_t such that $f(N_t)$ is maximized. The plot of $\text{SINR}_{\text{av}, b, \text{UB}}$ (red curve), η^p (blue curve) and $f(N_t)$ (green curve), as a function of N_t , keeping N_{tot} fixed, is depicted in **Fig. 2** and **3**. Note that $\text{SINR}_{\text{av}, b, \text{UB}}$ increases monotonically and η^p decreases monotonically, with increasing N_t . We also find that $f(N_t)$ has a minimum (not maximum) at

$$N_t = N_{\text{tot}} - 2N_{rt}\sqrt{N_{\text{tot}} - 1} \quad (17)$$

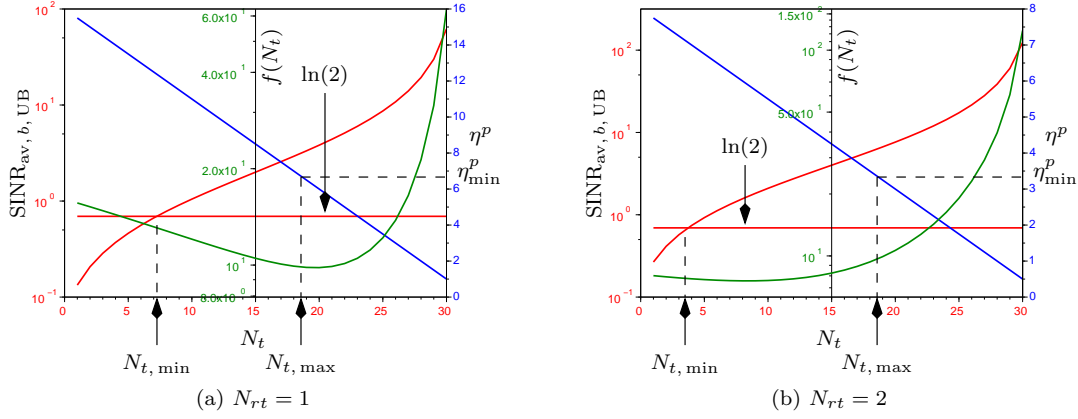


Fig. 3. $\text{SINR}_{\text{av},b,\text{UB}}$ and η^p as a function of N_t for $N_{\text{tot}} = 32$.

which is obtained by differentiating $f(N_t)$ in (16) with respect to N_t and setting the result to zero. Therefore, the only possible solution is to avoid the minimum. Clearly we require $\text{SINR}_{\text{av},b,\text{UB}} > \ln(2)$, since it is the minimum average SNR per bit required for error-free transmission over any type of channel [22]. We also require $\eta^p > \eta_{\text{min}}^p$, where η_{min}^p is chosen by the system designer. Thus, we arrive at a range of the number of transmit antennas ($N_{t,\text{min}} \leq N_t \leq N_{t,\text{max}}$) that can be used, as shown in **Fig. 2** and **3**. Note that in **Fig. 3(b)** the minimum of $f(N_t)$ cannot be avoided, since η_{min}^p would be too small.

Next, similar to (20) in [22], consider

$$\begin{aligned} \tilde{Y}_i &= \frac{1}{N_{rt}} \sum_{k=0}^{N_{rt}-1} \tilde{R}_{k,i} \\ &= \frac{1}{N_{rt}} \sum_{k=0}^{N_{rt}-1} (\tilde{F}_{k,i} S_i + \tilde{I}_{k,i} + \tilde{W}_{k,i}) \\ &= F_i S_i + \tilde{U}_i \quad \text{for } 1 \leq i \leq N_r \end{aligned} \quad (18)$$

where $\tilde{R}_{k,i}$ is given by (2), F_i is real-valued and

$$\begin{aligned} F_i &= \frac{1}{N_{rt}} \sum_{k=0}^{N_{rt}-1} \tilde{F}_{k,i} \\ \tilde{U}_i &= \frac{1}{N_{rt}} \sum_{k=0}^{N_{rt}-1} (\tilde{I}_{k,i} + \tilde{W}_{k,i}) \\ &= \frac{1}{N_{rt}} \sum_{k=0}^{N_{rt}-1} \tilde{U}'_{k,i} \quad (\text{say}). \end{aligned} \quad (19)$$

Since $\tilde{F}_{k,i}$ and $\tilde{U}'_{k,i}$ are statistically independent over re-transmissions (k), we have

$$\begin{aligned} E[F_i^2] &= \frac{1}{N_{rt}^2} E \left[\sum_{k=0}^{N_{rt}-1} \tilde{F}_{k,i} \sum_{n=0}^{N_{rt}-1} \tilde{F}_{n,i} \right] \\ &= \frac{4\sigma_H^4 N_t [N_t + 1 + N_t(N_{rt} - 1)]}{N_{rt}} \\ &= \frac{4\sigma_H^4 N_t (N_t N_{rt} + 1)}{N_{rt}} \end{aligned}$$

$$\begin{aligned} E \left[|\tilde{U}_i|^2 \right] &= \frac{\sigma_{\tilde{U}_i}^2}{N_{rt}} \\ &= \frac{8\sigma_H^4 N_t (N_r - 1) + 2\sigma_W^2}{N_{rt}} \end{aligned} \quad (20)$$

where we have used (4), (6), (11) and the fact that

$$E[\tilde{U}'_{k,i}] = 0 \quad (21)$$

where $\tilde{U}'_{k,i}$ is defined in (19). Next, we compute the average SINR per bit for \tilde{Y}_i in (18). Note that since \tilde{Y}_i is a ‘‘combination’’ of N_{rt} re-transmissions, its information content is $N_{rt}/(2N_{rt}) = 1/2$ bit (recall that the information content of $\tilde{R}_{k,i}$ in (18) is $1/(2N_{rt})$ bits). Therefore

$$\begin{aligned} \text{SINR}_{\text{av},b,C} &= \frac{E[|F_i S_i|^2] \times 2}{E[|\tilde{U}_i|^2]} \\ &= \frac{8\sigma_H^4 N_t (N_t N_{rt} + 1) \times 2}{8\sigma_H^4 N_t (N_r - 1) + 2\sigma_W^2} \end{aligned} \quad (22)$$

where the subscript ‘‘C’’ denotes ‘‘after combining’’ and we have used (8) and (20). Note that we prefer to use the word ‘‘combining’’ rather than averaging, since it is more appropriate in terms of the ‘‘information content’’ in \tilde{Y}_i . Once again with $\sigma_W^2 = 0$ and $N_t N_{rt} \gg 1$ we get the approximate upper bound on $\text{SINR}_{\text{av},b,C}$ as

$$\begin{aligned} \text{SINR}_{\text{av},b,C,\text{UB}} &= \frac{8\sigma_H^4 N_t (N_t N_{rt} + 1) \times 2}{8\sigma_H^4 N_t (N_r - 1)} \\ &\approx \frac{2N_{rt} N_t}{N_r - 1} \\ &\approx \text{SINR}_{\text{av},b,\text{UB}} \end{aligned} \quad (23)$$

when $N_t \gg 1$. Thus, the upper bound on the average SINR per bit before and after combining are nearly identical. Observe that re-transmitting the data increases the upper bound on the average SINR

per bit, it does not improve the BER performance, which is seen in the next section. After concatenation, the signal \tilde{Y}_i in (18) for $0 \leq i \leq L_d - 1$ is sent to the turbo decoder. The details of turbo decoding will not be discussed here.

4. Simulation Results

In this section, we discuss the results from computer simulations. The length of the data bits per “frame” (L_{d1}) is taken to be the smallest integer greater than 1000, which is an integer multiple of N_r . Note that (see Fig. 1)

$$L_d = 2L_{d1}. \quad (24)$$

The simulations were carried out over 10^4 frames. The turbo encoder is given by (38) of [22].

- **Fig. 4(a)** gives the bit-error-rate (BER) results for a 1×1 single input single output (SISO) system ($N_{\text{tot}} = 2$). We get a BER of 2×10^{-2} at an average SNR per bit of 3.5 dB, with $N_{rt} = 4$. The corresponding spectral efficiency is $\eta^p = 1/8$ bits per transmission. The BER also does not vary significantly with the number of re-transmissions (N_{rt}).
- **Fig. 4(b)** gives the results for $N_{\text{tot}} = 32$ and different combinations of transmit (N_t) and receive (N_r) antennas. We find that the BER is quite insensitive to variations in N_t , N_r and N_{rt} . Moreover, the BER at an SNR per bit of 3.5 dB is about 2×10^{-6} , which is a significant improvement over the SISO system. Of all the curves, $N_t = 25$, $N_{rt} = 2$ gives the lowest spectral efficiency of $\eta^p = 1.75$ bits/sec/Hz and highest $\text{SNR}_{\text{av}, b, \text{UB}} = 12.39$ dB. Of all the curves, $N_t = 12$, $N_{rt} = 1$ gives the highest spectral efficiency $\eta^p = 10$ bits/sec/Hz and lowest $\text{SNR}_{\text{av}, b, \text{UB}} = 1.36$ dB.
- **Fig. 4(c)** gives the results for $N_{\text{tot}} = 1024$ for various combinations of N_t , N_r and N_{rt} . The BER is similar to that of $N_{\text{tot}} = 32$. Of all the curves, $N_t = 400$, $N_{rt} = 1$ gives the highest spectral efficiency of $\eta^p = 312$ bits/sec/Hz and lowest $\text{SNR}_{\text{av}, b, \text{UB}} = 1.09$ dB. Of all the curves, $N_t = 1023$, $N_{rt} = 2$ gives the lowest spectral efficiency of $\eta^p = 0.25$ and highest $\text{SNR}_{\text{av}, b, \text{UB}} \rightarrow \infty$.

5. Conclusions

This work presents a method for data detection in turbo-coded and precoded massive MIMO. An ideal receiver is assumed. Future work could be to simulate a realistic precoded system with carrier and timing synchronization and channel estimation.

References

- [1] R. W. Chang, “Precoding for multiple-speed data transmission,” *The Bell System Technical Journal*, vol. 46, no. 7, pp. 1633–1649, Sep. 1967.
- [2] S. Kasturia and J. M. Cioffi, “Precoding for blocking signalling and shaped signal sets,” in *IEEE International Conference on Communications, World Prosperity Through Communications*, June 1989, pp. 1086–1090 vol.2.
- [3] G. J. Pottie and M. V. Eyuboglu, “Combined coding and precoding for pam and qam hds1 systems,” *IEEE Journal on Selected Areas in Communications*, vol. 9, no. 6, pp. 861–870, Aug 1991.
- [4] A. K. Aman, R. L. Cupo, and N. A. Zervos, “Combined trellis coding and dfe through tomlinson precoding,” *IEEE Journal on Selected Areas in Communications*, vol. 9, no. 6, pp. 876–884, Aug 1991.
- [5] G. D. Forney and M. V. Eyuboglu, “Combined equalization and coding using precoding,” *IEEE Communications Magazine*, vol. 29, no. 12, pp. 25–34, Dec 1991.
- [6] M. V. Eyuboglu and G. D. Forney, “Trellis precoding: combined coding, precoding and shaping for intersymbol interference channels,” *IEEE Transactions on Information Theory*, vol. 38, no. 2, pp. 301–314, 1992.
- [7] R. Laroia, S. A. Tretter, and N. Farvardin, “A simple and effective precoding scheme for noise whitening on intersymbol interference channels,” *IEEE Transactions on Communications*, vol. 41, no. 10, pp. 1460–1463, 1993.
- [8] H. W. Bode, “Variable equalizers,” *The Bell System Technical Journal*, vol. 17, no. 2, pp. 229–244, 1938.
- [9] S. U. H. Qureshi, “Adaptive equalization,” *Proceedings of the IEEE*, vol. 73, no. 9, pp. 1349–1387, 1985.
- [10] K. Vasudevan, “Detection of signals in correlated interference using a predictive va,” in *The 8th International Conference on Communication Systems, 2002. ICCS 2002.*, vol. 1, 2002, pp. 529–533 vol.1.
- [11] K. Vasudevan, “Detection of signals in correlated interference using a predictive va,” *Signal Processing*, vol. 84, no. 12, pp. 2271 – 2286, 2004, [Online].
- [12] R. Koetter, A. C. Singer, and M. Tüchler, “Turbo Equalization,” *IEEE Sig. Proc. Mag.*, vol. 21, no. 1, pp. 67–80, Jan. 2004.
- [13] K. Vasudevan, “Turbo Equalization of Serially Concatenated Turbo Codes using a Predictive DFE-based Receiver,” *Signal, Image and Video Processing*, vol. 1, no. 3, pp. 239–252, Aug. 2007.
- [14] —, *Digital Communications and Signal Processing, Second edition (CDROM included)*. Universities Press (India), Hyderabad, www.universitiespress.com, 2010.
- [15] N. Fatema, G. Hua, Y. Xiang, D. Peng, and I. Natgunanathan, “Massive mimo linear precoding: A survey,” *IEEE Systems Journal*, vol. 12, no. 4, pp. 3920–3931, Dec 2018.
- [16] S. Kim, “Diversity order of precoding-aided spatial modulation using receive antenna selection,” *Electronics Letters*, vol. 56, no. 5, pp. 260–262, 2020.
- [17] —, “Transmit antenna selection for precoding-aided spatial modulation,” *IEEE Access*, vol. 8, pp. 40 723–40 731, 2020.
- [18] A. Haqiqatnejad, F. Kayhan, and B. Ottersten, “Robust sinr-constrained symbol-level multiuser precoding with imperfect channel knowledge,” *IEEE Transactions on Signal Processing*, vol. 68, pp. 1837–1852, 2020.
- [19] Q. Deng, X. Liang, X. Wang, M. Huang, C. Dong, and Y. Zhang, “Fast converging iterative precoding for massive mimo systems: An accelerated weighted neumann series-steepest descent approach,” *IEEE Access*, vol. 8, pp. 50 244–50 255, 2020.
- [20] Z. Li, C. Zhang, I. Lu, and X. Jia, “Hybrid precoding using out-of-band spatial information for multi-user multi-rf-chain millimeter wave systems,” *IEEE Access*, vol. 8, pp. 50 872–50 883, 2020.

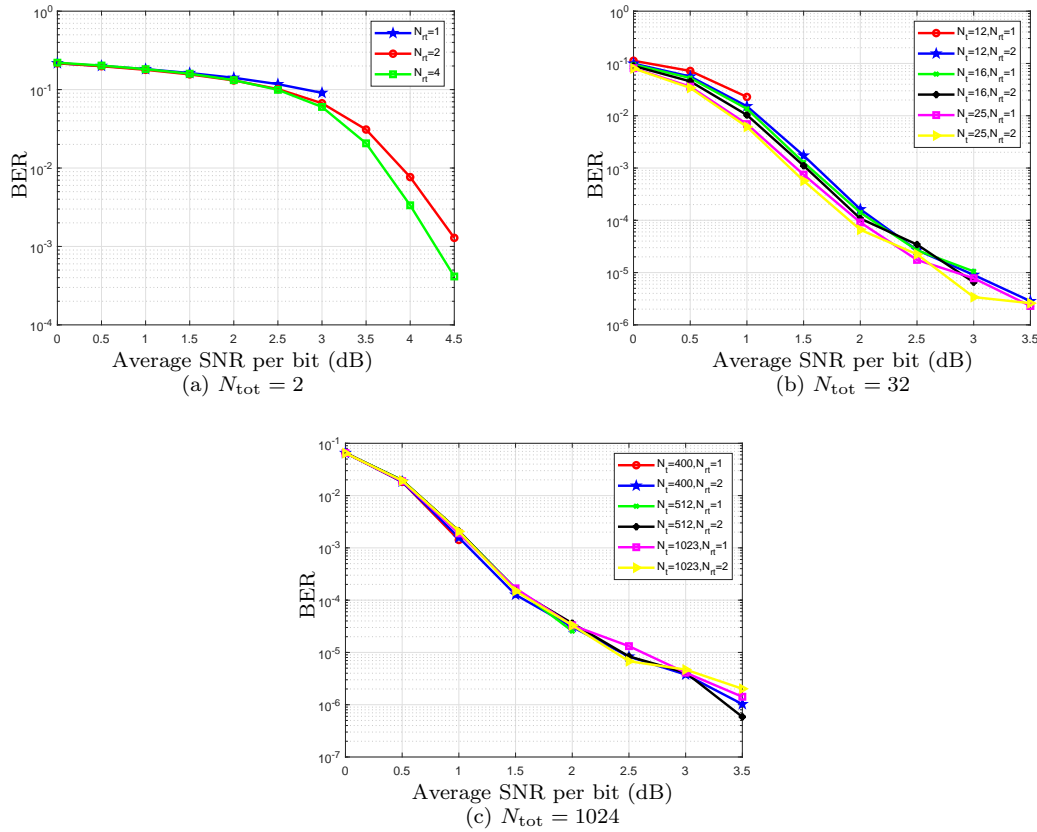


Fig. 4. Simulation results.

- [21] N. L. Johannsen, N. Peitzmeier, P. A. Hoeher, and D. Manteuffel, "On the feasibility of multi-mode antennas in uwb and iot applications below 10 ghz," *IEEE Communications Magazine*, vol. 58, no. 3, pp. 69–75, 2020.
- [22] K. Vasudevan, K. Madhu, and S. Singh, "Data Detection in Single User Massive MIMO Using Re-Transmissions," *The Open Signal Processing Journal*, vol. 6, pp. 15–26, Mar. 2019.
- [23] K. Vasudevan, S. Singh, and A. P. K. Reddy, "Coherent receiver for turbo coded single-user massive mimo-ofdm with retransmissions," in *Multiplexing*, S. Mohamady, Ed. London: IntechOpen, 2019, ch. 4, pp. 1–21.
- [24] U. C. Samal and K. Vasudevan, "Preamble-based timing synchronization for ofdm systems," in *2013 3rd IEEE International Advance Computing Conference (IACC)*, Feb. 2013, pp. 313–318.
- [25] K. Vasudevan, "Coherent detection of turbo coded ofdm signals transmitted through frequency selective rayleigh fading channels," in *Signal Processing, Computing and Control (ISPC), 2013 IEEE International Conference on*, Sept. 2013, pp. 1–6.
- [26] D. V. Adakane and K. Vasudevan, "An efficient pilot pattern design for channel estimation in ofdm systems," in *2013 IEEE International Conference on Signal Processing, Computing and Control (ISPC)*, Sept. 2013, pp. 1–5.
- [27] U. C. Samal and K. Vasudevan, "Bandwidth efficient turbo coded ofdm systems," in *2013 13th International Conference on ITS Telecommunications (ITST)*, Nov. 2013, pp. 493–498.
- [28] K. Vasudevan, "Coherent detection of turbo-coded ofdm signals transmitted through frequency selective rayleigh fading channels with receiver diversity and increased throughput," *Wireless Personal Communica-*
- tions*, vol. 82, no. 3, pp. 1623–1642, 2015. [Online]. Available: <http://dx.doi.org/10.1007/s11277-015-2303-8>
- [29] —, "Coherent turbo coded mimo ofdm," in *ICWMC 2016, The 12th International Conference on Wireless and Mobile Communications*, Nov. 2016, pp. 91–99, [Online].
- [30] —, "Near capacity signaling over fading channels using coherent turbo coded ofdm and massive mimo," *International Journal On Advances in Telecommunications*, vol. 10, no. 1 & 2, pp. 22–37, 2017, [Online].
- [31] —, "Scilab code for coherent detection of turbo coded ofdm signals transmitted through frequency selective rayleigh fading channels," <https://www.codeocean.com/>, 7 2019.
- [32] K. Vasudevan, K. Madhu, and S. Singh, "Scilab code for data detection in single user massive mimo using re-transmissions," <https://www.codeocean.com/>, 6 2019.
- [33] K. Vasudevan, S. Singh, and A. P. K. Reddy, "Scilab code for coherent receiver for turbo coded single-user massive mimo-ofdm with retransmissions," <https://www.codeocean.com/>, 6 2019.
- [34] K. Vasudevan, A. Phani Kumar Reddy, G. K. Pathak, and S. Singh, "On the probability of erasure for mimo ofdm," *Semiconductor Science and Information Devices*, vol. 2, no. 1, pp. 1–5, Apr. 2020.
- [35] K. Vasudevan, A. P. K. Reddy, G. K. Pathak, and S. Singh, "Scilab code for the probability of erasure for mimo-ofdm," <https://www.codeocean.com/>, 4 2020.
- [36] A. Papoulis, *Probability, Random Variables and Stochastic Processes*, 3rd ed. McGraw-Hill, 1991.
- [37] K. Vasudevan, *Analog Communications: Problems & Solutions*. Ane Books, 2018.